Applied Energy Symposium 2020: Low carbon cities and urban energy systems
October 10-17, 2020
Paper ID: D040

Improve the charge and discharge performance of vanadium redox flow battery by thermal spraying CNT on the surface of the positive and negative carbon materials

Zhongxu Tai[1], Susumu Sato[1], Wenping Luo[1], Kenzo Hanawa[4],Dongying Ju[1,2,3,4*]

1 Department of Information System, Saitama Institute of Technology, Japan

2 Advanced Science Institute, Saitama Institute of Technology, Japan

3 Ningbo Haizhi Institute of Material Industry Innovation, China

4 Tokyo Green Power Electric Research Institute Co.,Ltd

ABSTRACT

The Carbon fiber electrode is a cathode material in all-vanadium flow battery. In order to further reduce the volume of the all-vanadium power storage system, further reduce the internal resistance of the carbon fiber electrode, increase the current density of the electrode, and achieve high electrical conductivity and large electrostatic capacitance are essential. Among them, the graphitization of the positive electrode material and the improvement of the specific surface area of the electrode surface also greatly affect the performance of the all-vanadium redox flow battery. Therefore, in this paper, carbon nanotubes (CNTs) with small diameter and large specific surface area are thermal plated on the surface of conventional carbon fibers, and the specific resistance can be reduced to almost half by increasing the specific surface area of the carbon fibers. The charge and discharge experiments of the all-vanadium flow battery prove that this method is very effective to improve the performance of the all-vanadium flow battery.

Keywords: forredox battery electrodes electrolyte carbon fiber

1. INTRODUCTION

The flow battery is an electrochemical energy storage technique proposed by Thaller (NASA Lewis Research Center, Cleveland, United States) in 1974[1.2].The flow battery is also referred to as a battery active material regenerative fuel cell [3]. When vanadium ions are used as the active material of the battery, while the system is working, the vanadium electrolyte in the liquid storage tank is pressed into the battery stack by an external pump to complete the electrochemical reaction. In the positive electrode, the tetravalent vanadium ions are oxidized during charging. It is oxidized to pentavalent ions, and in the negative electrode, trivalent vanadium ions are reduced to divalent vanadium ions. This reverse reaction occurs during discharge. This reaction is as follows：

Positive electrode reaction:

$$VO^{2+} + H_2\ O \underset{\text{discharge}}{\overset{\text{charge}}{\rightleftarrows}} VO_2^{+} + e^- + 2H^+ \ \text{at}\ E^0 = +1.0V \quad (1)$$

Negative electrode reaction:

$$V^{3+} + e^- \underset{\text{discharge}}{\overset{\text{charge}}{\rightleftarrows}} V^{2+} \qquad \text{at}\ E^0 = -0.26V \quad (2)$$

Due to its high safety and long service life, vanadium flow batteries have been widely used in many fields. However, since the energy density is low, the floor space and the volume are large, so that it is difficult to be popularized. This time, we have obtained a few hundred mA/cm^2 (several hundred mW /cm$^{2)}$ of input/output by performing CNTs modification and heat treatment on the surface of the carbon fiber electrode of the battery for the high output of the all-vanadium flow battery. density. Furthermore, the use of a common battery active material for each unit cell enables simplification of the battery system including the regulator, and allows the construction of a storage system capable of handling irregular multiple inputs and outputs.

In general, there are many factors that affect the performance of carbon fiber electrodes [4]. This paper describes that the specific surface area of carbon fibers is increased by the carbon nanotube dispersion treatment and hot-dip method, which reduces the resistance of the carbon fiber electrode and improves

Selection and peer-review under responsibility of the scientific committee of CUE2020

the conductivity of the electrode. Moreover, the carbon fiber electrode is further heat treated to promote the graphitization of the electrode and improve the conductivity of the electrode. The improved cathode material was used in the all-vanadium flow battery system, and the effectiveness of this method was verified by charge and discharge experiments

2. EXPERIMENTAL METHOD

2.1 CNTs dispersion coating and heat treatment

Since the discovery of carbon nanotubes by Iijima, S in 1991 and 1993[5.6], its unique performance and potential application value have attracted widespread attention, research and application[7]. At present, the dispersion method of carbon nanotubes mainly includes two types of physical dispersion methods and chemical dispersion methods. The physical dispersion method mainly includes milling, ball milling, ultrasonic wave, etc.; the chemical dispersion method mainly includes the addition of a surfactant, a strong acid and a strong alkali washing, etc.; in addition, an in-situ synthesis method can be used to prepare a carbon nanotube composite material. Due to the grinding and strong acid and alkali washing methods, the CNTs structure is destroyed and the original performance is lowered. Therefore, this time we dispersed the CNTs by adding a surfactant and ultrasonic dispersion.

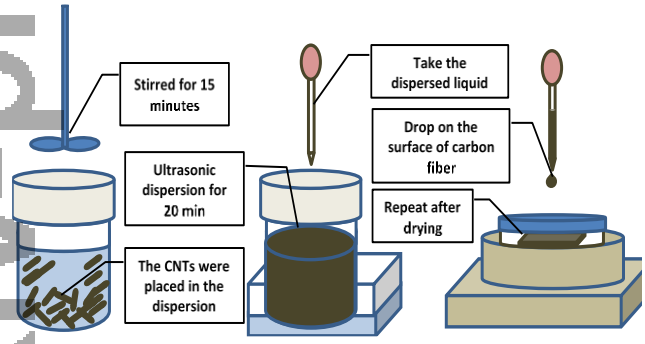

FIG. 1. CNTs dispersion and carbon fiber modification

The CNTs used in this experiment were multi-walled carbon nanotubes manufactured by WACO Chemical, which had commercially available multi-walled CNTs with an average diameter of 10 nm and an average length of 1 μm. The dispersion medium mainly contains deionized water and ethanol solution, and the surfactant is SDBS (sodium dodecyl benzenesul fonate). Here, 0.006g of CNTs was placed in three different solvents, stirred for 15 min, sonicated for 20 min, and allowed to stand for 1 h. The stability of the solution after dispersion was determined by measuring the ZETA potential. The surface-modified carbon fiber electrode was placed in a tubular vacuum furnace, and the carbon fiber electrode was heat-treated at different temperatures to compare its charge and discharge performance. There are two methods for evaluating the treated carbon fibers.

In the heat treatment part of this experiment, the modified carbon fibber electrode was heat treated by a tubular vacuum furnace, the degree of vacuum was 10^{-2}-10^{-3}pa, and the maximum temperature was from 800 °C to 1500 °C. After one hour, keep it for one hour, then take it out when the furnace is cooled to 200 °C.

2.2 *Evaluation and analysis of electrode performance after coating*

The surface state and elements of the carbon fiber electrode were observed and analyzed by SEM-EDS. Charge and discharge experiment and measurement of AC resistance By comparing the charge and discharge characteristics of carbon fiber electrodes after the small battery test, the impedance of the battery body was tested, and the internal resistance was compared. The battery size for the test is shown in Figure 2.

For the difference of charge and discharge

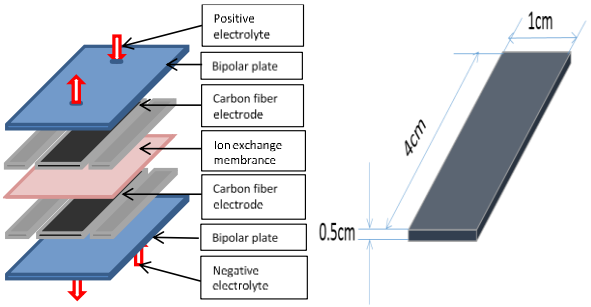

FIG. 2. Battery model and electrode size for test

performance, the surface of the carbon fibber electrode was observed and analyzed by SEM-EDS. The degree of graphitization of the carbon fibber electrode was evaluated by Raman spectroscopy of the Raman spectrometry electrode for the D peak at 1360 cm-1 and the G integral area ratio ID/IG at 1580cm-1. Analysis of crystallization of treated electrode by XRD.

3. EXPERIMENTAL RESULTS AND DISCUSSION

3.1 The dispersion and surface observation of carbon nanotubes in the coating

The dispersion of the three dispersions at different concentrations was compared by measuring the ZETA potential. The results showed that the dispersion of 80%

ethanol solution, 0.1mol/L SDBS aqueous solution and 0.1mol/L (SDBS+80% Ethanol) solution was the best. The measured results are shown in Fig. 3.Since a large amount of bubbles were generated after the ultrasonic treatment of the SDBS ethanol solution, the solution began to stand after standing for 2 hours, and the precipitate was apparent after standing for six hours.

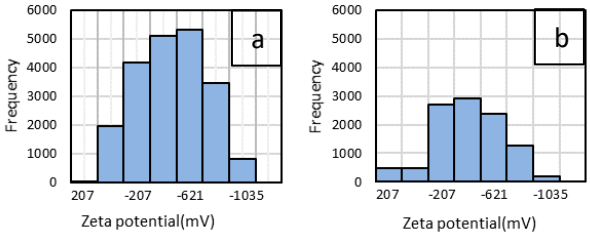

FIG. 3. 80% ethanol solution(a)and0.1mol/L(SDBS+80%Ethanol) (b)

Therefore, this experiment used 80% ethanol solution.

3.2 SEM-EDS surface observation and element analysis

FIG.4 shows the SEM images of the untreated carbon fiber electrode (abc), the CNT carbon fiber electrode (def) directly added under heat treatment at 1000°C and

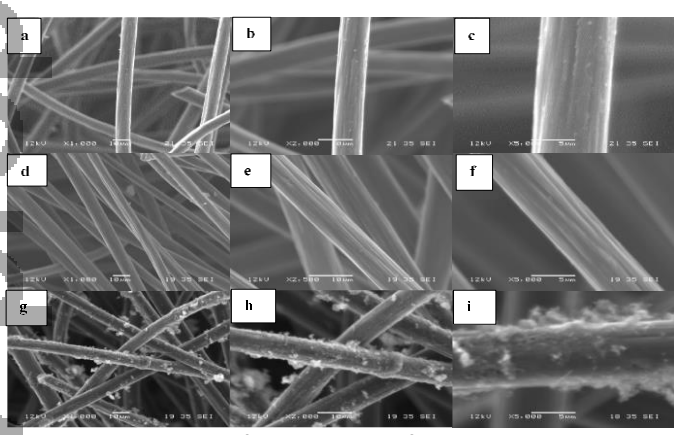

FIG.4. Comparison of SEM images of untreated electrodes, heat treated electrodes at 1000 °C and heat treated electrodes at 1000 °C after CNT modification.
（abc:Untreated carbon fiber electrode,def: Undispersed CNTs 1000°C heat-treated carbon fiber electrode,ghi:1000°C heat treatment carbon fiber electrode after CNTs are dispersed）

the carbon fiber electrode (ghi) after addition dispersion after heat treatment at 1000°C. As can be seen from FIG.4b and FIG.4c, the untreated electrode has a smooth surface with a diameter of about 9 μm.On the electrode after heat treatment at 1000°C, it can be seen from FIG.4e and FIG.4f that the surface has obvious gully marks and the diameter is about 7μm. FIG.4h and FIG.4i show the surface-modified heat-treated electrode, and the adhesion of the CNTs on the electrode surface can be clearly seen, and the electrode diameter is about 8μm. The effects of heat treatment and surface modification on the electrode surface under different conditions were confirmed by SEM image comparison. The heat-treated electrode has obvious gully marks due to oxidative etching of the electrode surface. After modification by CNTs, the specific surface area of the electrode is greatly increased.

The surface element analysis of untreated carbon fiber electrode (a), carbon fiber electrode with CNTs undispersed and heat treated at 1000℃ (b) and carbon fiber electrode with CNTs dispersed after 1000℃ heat treatment is shown in FIG.5. And Table 1 is shown. The O/C of the surface of the carbon fiber electrode after heat treatment is larger than that of the untreated electrode and the surface modified carbon fiber electrode. The reason for this is that the heat treatment causes an oxidation reaction on the surface of the carbon fiber electrode, and the active specific surface area of the surface containing active bonds C—O and C=O is increased[8].

Table 1. EDS surface element analysis results comparison

	C Ka(%)	O Ka (%)	Al La (%)	Si Ka (%)	O/C
A	86.53	2.5	4.8	4.5	0.02
B	75.73	4.8	5.3	15.38	0.06
C	81.62	3.7	6.12	8.16	0.04

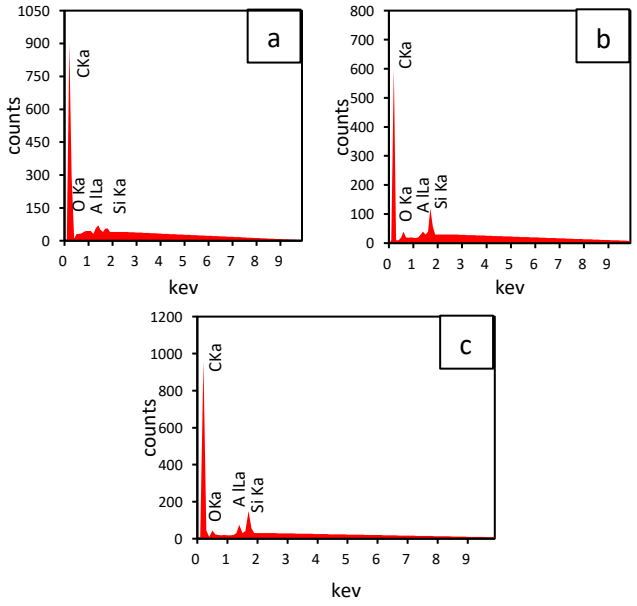

FIG.5. EDS surface element analysis results （a：Untreated carbon fiber electrode，b： Undispersed CNTs 1000°C heat-treated carbon fiber electrode，c：1000°C heat treatment carbon fiber electrode after CNTs are dispersed）

3.3 Performance evaluation

Through charge-discharge experiment and measurement of AC resistance, the impedance of the battery body was tested by comparing the charge-discharge characteristics of the carbon fiber electrode after the small battery test, and the internal resistance was compared.

According to the 2A constant current charge and discharge data, the properties of the carbon fibber electrode after each temperature treatment were calculated. As shown in Table 2, the internal resistance of the electrode after heat treatment at 1000°C was reduced by 30% compared with the untreated electrode. Coulombic efficiency increased by 10%, voltage efficiency increased by 15%, and energy efficiency increased by 20%. According to the calculated data, the current density is summarized. The relationship between the volumetric power densityand the discharge voltage is shown in FIG.7. When the current density reaches 1000 mA/cm^2, the volumetric power densityis the largest, which is 930 W/L.

The purpose of this study was to miniaturize the redox flow battery, reduce costs, and increase input/output. Now, the redox flow batteries are bulky, expensive, and have low current densities. In according to the results of the study， the electrode treated at 1000°C has a maximum current density exceeding 1000mA/cm^2 . It is more than three times the current density of a conventional vanadium redox flow battery. The charge and discharge results are shown in FIG 6. From performance of the charge and discharge， we can known the electrode heat treated at 1000°C is optimal for high speed charging and discharging, but the voltage is divided into two stages from the discharge curve at low speed charging and discharging. Low speed charge and discharge performance deteriorates. Consider the reason. In this experiment, the charge and discharge tests were performed with the pump stopped. The adsorption performance of CNTs is higher than that of carbon fibers. $V5^+$ is first adsorbed on the CNTs. The first platform voltage is the voltage of $V5^+$ and $V2^+$. The reaction continues and when $V5^+$ is fully reacted, the

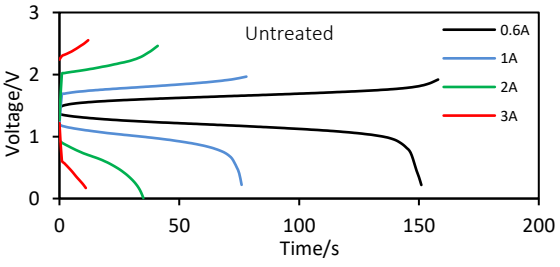

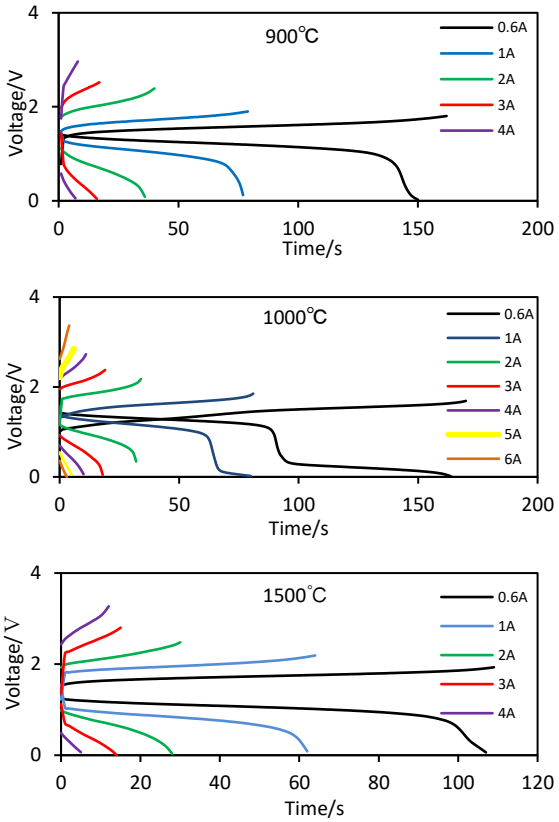

FIG.6. Charge and discharge data

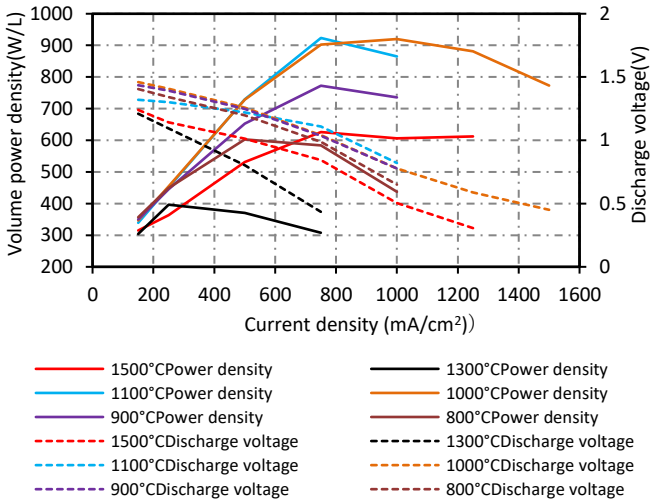

FIG.7. Relationship between discharge current density, discharge electric power and volumetric force density

Table 2. 2A constant current charge and discharge data comparison

2Acharge and discharge test	Untreated	900°C	1000°C	1500°C
Internal resistance(Ωcm^2)	1.5	1.051	1.01	1.49
Coulombic efficiency(%)	85	90.9	97	90.32
Voltage efficiency(%)	30	38.5	47.5	30.15
Energy efficiency(%)	25	34.99	46.07	27.23

second platform is the reaction voltage of V^{4+} and V^{2+}.For this reason, the low rate discharge curve is divided into two segments.

As a result of the charge and discharge data, the battery was subjected to an alternating Impedance measurement, and the measured result (Nyquist diagram) is shown in Fig 8. The test range is 10^5 Hz → 0.1 Hz. The intersection of the curve starting position and the x-axis is the conduction resistance (RL) of the battery itself. In the figure, the semi-circular portion is the high-frequency region charge moving resistance (RP), and the oblique line portion is the low-frequency region material moving resistance (RD). This experiment mainly reviews the reaction resistance (RP+ RD) when a redox reaction occurs in the high frequency region and the low frequency region[9]. The resistance of each electrode was calculated according to the measured Nyquist

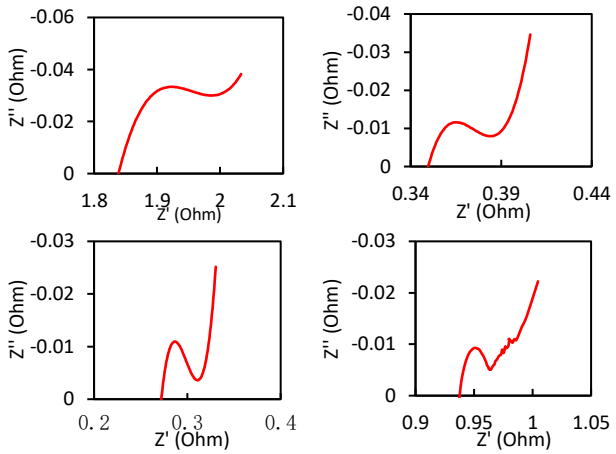

FIG.8. Single battery cell Nyquist figure

Table 3.Breakdown of small cell resistance component estimated from Nyquist diagram

	Untreated	800°C	900°C	1000°C	1100°C	1200°C	1300°C	1400°C	1500°C
Ohmic（Ω）	1.83	0.34	0.35	0.27	3.84	3.76	0.72	1.83	0.94
Charge transfer（Ω）	0.17	0.07	0.04	0.03	0.03	0.04	0.03	0.03	0.02
Mass transfer（Ω）	0.05	0.1	0.04	0.01	0.05	0.03	0.04	0.01	0.03
Total（Ω）	2.05	0.52	0.43	0.31	3.92	3.83	0.79	1.87	0.99

diagram. As shown in Table 3, the cell reaction resistance of the carbon fibber electrode after surface modification and heat treatment at 1000°C was 0.04 Ω, which was much smaller than 0.22 Ω of the untreated electrode. The reason for the analysis is that the addition of CNTs can lower the reaction resistance of the electrode and promote the occurrence of redox reaction of the electrolyte.

3.4 Raman spectroscopic detection and XRD surface crystallization analysis

The Raman spectroscopic and XRD crystal structure analysis of the untreated and treated electrodes was carried out for the difference between the electrode charge and discharge and the AC Impedance results.

In this paper, a common method used for the analysis of carbon materials by Raman spectroscopic spectroscopy. There are two characteristic peaks in the Raman spectrum of carbon materials: the G peak near 1580cm^{-1} and the D peak near 1360cm^{-1}[10]. The researchers usually pass the D peak and the G peak. The integrated area ratio ID/IG used to determine the integrity of the carbon material. The larger the value of the ID/IG ratio, the lower the structural integrity of the carbon material. The smaller the value of the ID/IG ratio, the higher the structural integrity of the carbon material[11.12]. In this study, the Raman spectroscopic test was performed on the treated carbon fiber electrode using NRS-4100 of JASCO Corporation. The measured Raman spectroscopic spectrum is shown in FIG.9, and the measured data is shown in Table 4.

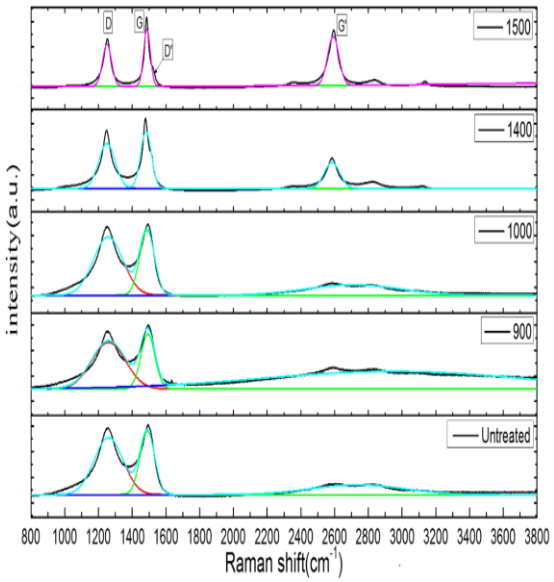

FIG. 9.Structural analysis result by Raman spectroscopy

Combined with Raman spectroscopy and measured data, it can be seen that as the heat treatment temperature increases, the peak shapes of the D and G peaks become relatively sharp and distinct, and the integrated area ratio and the full width at half maximum of the peak are also smaller. When the temperature reached 1400°C, the characteristic peak G' of graphite in the vicinity of 2700 cm^{-1} became apparent. The intensity of the G' peak also increases with increasing temperature. Based on the above data, it can be consider that the heat treatment can effectively improve the structural integrity of the carbon fiber electrode.

Table 4. Surface observation and analysis result summary

Sample	D peak		G peak		ID/IG（Area）
	Raman shift/ cm^{-1}	FWHM/ cm^{-1}	Raman shift/ cm^{-1}	FWHM/ cm^{-1}	
Untreated	1255	71.90	1491	52.01	1.038
900°C	1252	106.24	1494	87.33	1.019
1000°C	1252	256.12	1494	124.08	1.012
1400°C	1247	433.56	1477	161.95	1
1500°C	1252	307.33	1487	147.81	0.97

For the surface crystal structure, untreated and treated carbon fibbers were analysed using RINT 2500 VHF from RIGAKU Co., Ltd., and the test conditions were as follows: voltage: 40 kV: 30 mA (Cu). The measured results are shown in FIG. 10. It can be seen that the (002) diffraction peak shape of 2θ = 25° is substantially the same. However, the peak intensity after heat treatment at 1500°C increased. There is no significant difference in the (100) diffraction peak at 2θ = 43°.

$$d_{002} = \frac{\lambda}{2sin\theta} \quad (3)$$

$$L = \frac{K\lambda}{\beta cos\theta} \quad (4)$$

According to formula (3) and formula (4), the layer spacing d002 of the carbon fibber graphite crystallites and the thickness of the crystallite stack Lc can be calculated[13]. The (100) peak in the XRD spectrum can be used to calculate the direction of the graphite crystallite along the axis. The crystal plane width La. The diffraction angle of the θ crystal plane diffraction peak; λ is the wavelength (λ = 0.1541nm); K is the shape factor, K = 0.94 when Lc is calculated, and K = 1.84 when La is calculated; β is the measured full width at half maximum. The calculation results are shown in Table 5.

From the comparison of the calculation results in Table 5, it is found that there is no significant difference between crystal spacing d002 and crystal spacing d100 of the untreated and treated electrodes; as the heat treatment temperature increases, the carbon fibber electrode is slightly The crystal radial dimension Lc and the axial dimension La become larger. The size of the

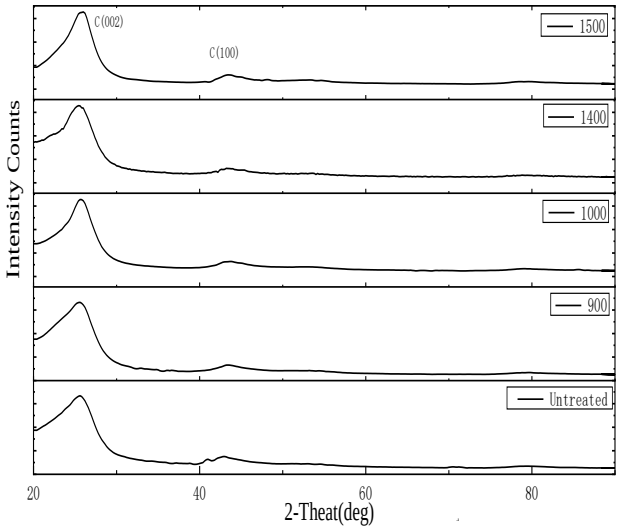

FIG. 10.Crystal Structure Analysis Results of XRD at Different Temperatures

Table 5. XRD pattern of carbon fiber after surface treatment at different temperatures

CF	C(002) crystallographic plane				C(100) crystallographic plane			
	2θ /°	d/nm	β /rad	Lc /nm	2θ /°	d/nm	β /rad	La /nm
Untreated	25.6	0.356	0.141	1.054	42.8	0.228	1.385	0.221
900°C	25.6	0.356	0.130	1.143	43.6	0.225	1.334	0.229
1000°C	25.8	0.354	0.121	1.221	43.4	0.224	1.310	0.233
1400°C	25.6	0.356	0.133	1.117	43.6	0.225	1.330	0.229
1500°C	25.8	0.354	0.100	1.488	43.4	0.224	1.237	0.246

crystallites becomes larger, indicating that development is more complete and the degree of graphitization is higher[14]. It is thus theoretically demonstrated that the performance of the treated carbon fibber electrode is higher than that of the untreated electrode.

4. CONCLUSION

After the CNTs wear dispersed on the surface of the carbon fibber, the charge and discharge current density reached 1000A/cm^2. Compared with the untreated electrode, the charge and discharge performance wear improved by about 15%. The Impedance test results show that the charge transfer resistance and mass shift resistance of the battery are reduced by 0.18Ω. SEM-EDS confirmed the surface state and elemental composition of the modified carbon fiber electrode.

For the improvement of charge and discharge performance, the carbon fiber electrode was analyzed by Raman spectrometry and XRD crystal structure. The Raman spectroscopy results show that the integral area ratio of ID/IG becomes smaller as the heat treatment temperature increases, and the integrity of the carbon material is higher. The results of XRD analysis show that the heat treatment temperature increases, and the carbon fiber electrode has a larger crystallite radial dimension Lc and an axial dimension La. The crystallite size becomes larger and the degree of graphitization is higher. It is thus theoretically demonstrated that the performance of the treated carbon fiber electrode is higher than that of the untreated electrode.

ACKNOWLEDGEMENT

We thank Prof. Osamu Hamamoto for comments that greatly improved the manuscript.

REFERENCE

[1] Thallerl H, Nice A W. Fluid battery prom ises economical storage[J]. Power Engineering, 85(2):56-58, 1981.

[2] Thaller L H Electrically Rechangeable Redox Flow Cells [C]. San Francisco, USA:SAE Prep rints,749142. 924, 1974.

[3] Shunichi Uchiyama. Multipurpose redox flow battery. Development trend of redox flow battery. CMC publishing. 162-175, 2017.

[4] YANG Deng-lian, TIAN jiang. Factors Affecting the Performance of Super Activated Carbon Electrode[J]. Shihezi Technology, (1): 31-34, 2012

[5] lijima, S , Helical Microtubles of Graphic Carbonu)Nature,1991,354:56-58

[6] lijima, S, Ichihashi, T. Single-shell Carbon Nanotubesof 1-nm Diameteru) Nature,363: 603-605, 1993.

[7] Colvin, V L. The Potential Environmental Impact of EngineeredNanomaterials[J].NatureBiotechnology,21:1 166-1170,2003.

[8] STEFANICK K M. Laser welded lightweight sandwich panel fabrication and shipyard applications]. Concurrent Technologies Corporation. [S 1]: [s n]. 2005.

[9] Masaru Kobayashi. Carbon electrode. Development trend of redox flow battery. CMC publishing.126-137. 2017.

[10] Tuinstra F, Koenig J L. Characterization of graphite fiber surfaces with Raman spectroscopy D], Joumal of Composite Materials, 4(4) :492-499, 1970.

[11] Nakamizo M, Honda H, Inagaki M. Raman spectra of ground natural graphite [I. Caron. 16(4):281-283, 1978.

[12] Nemanich R J, Solin S A. First and second-order Raman seattering from finite-size crystals of graphite O]. Phys Rev, B20(2): 39240. 1979.

[13] Gong Wei. SVM method research on humid and hot aging for carbon fiber composite material in military equipment[J]. Journal of Sichuan Ordnance,(1):1-4. ,2011.

[14] Jing Min.Comparison of the Microstructure of Toray T800H and T800S Carbon Fibers[J].Materials Science and Technology (23),2:45-52,2015.